Optical Methods applied to Transient Heat Transfer and Two-Phase Flow

F. Mayinger, P. Gebhard

TU München, Lehrstuhl A für Thermodynamik, 80290 München, Germany

1. Introduction

Optical methods have a long tradition in heat transfer, their application to two-phase flow started much later. Their instant signals make them specially suited to transient situations provided that the registration method is quick enough and has a high sampling frequency.

A further benefit of optical methods is their non-invasive mode of operation, not interacting with the material to be investigated and by this not affecting the physical process under study.

Optical methods are using changes of light waves as sensoric signals, which are due to interaction between the light and the material. Such changes and interaction consequences can be

- attenuation,
- scattering,
- deflection or
- reflection.

Depending on the mode of registration we distinguish between

- image-forming and
- non-image-forming

methods. The latter ones allow only a spotwise record of the events and the first one is registering usually a two-dimensional picture of situations or processes on a surface or in a volume as well-known from photography. Since approximately twenty years a new image-forming method is in use, the holography, which found admission to measuring techniques in heat and mass transfer and two-phase flow in the last ten years. This holography is using two-dimensional registration tools, namely photographic plates, from which however three-dimensional information can be reconstructed. This has special advantages for studies of transient two-phase flow.

Holography combined with the well-known interferometry using the phase-shift of the light wave allows the registration of temperature- and concentration fields, and by this became a very valuable tool in heat and mass transfer.

From the spotwise working methods the Phase-Doppler-Anemometry, a modification of the Laser-Doppler-Anemometry is best known from the literature for two-phase flow application in dispersed flow. Mie-scattering is another method used in two-phase flow for example to detect spray characteristics.

It is not possible to present all optical methods being used in heat transfer and two-phase flow within a given time and a limited space. Even the concentration of such a survey on optical methods being applicable to transient conditions would cover a wide field of different techniques. Therefore, the author apologises for restricting this presentation on optical methods with which he has a longer experience and to which he contributed to their development to a certain extent.

2. Photography

Usually photographs are taken rectangular to the flow direction through a transparent wall made of glass, for example. With this special technique, however, disturbances and even falsifications have to be expected by the liquid film flowing along the wall. Therefore, Arnold and Hewitt /1/ proposed another method which takes photographs of two-phase mixture coaxially to the flow. This method is the only one of the techniques known which allows also to make clearly outlined pictures of very highly transient processes. A sketch of the optical arrangement is shown in Fig.1a. Langner /2/ altered this arrangement in some details, as shown in Fig.1b.

At the end of an electrically heated tube a flow splitter is placed which allows a separation of the liquid film at the wall and the gas core in the center entrained with droplets. At the top of the flow separator a lense is placed through which the flow can be observed, photographed or filmed in axial direction. The lense must be manufactured very precisely by using glass of high quality to avoid reflections. Following the heated test section a short glass tube is arranged through which the fluid can be illuminated from outside. The transition between heated steel tube and glass tube has to be smoothed very carefully to avoid disturbances of the flow.

The advantage of this special technique versus the usual methods photographing rectangular to the flow is demonstrated in Fig.2. The view from the top into the tube offers clear information about the radial droplet distribution and droplet form.

As "registration apparatus" a usual camera or any high-speed movie-camera can be used. Both types of cameras, however, need a focussing screen in the form of a ground glass to control the range within the tube in which a visual observation is intended. Missing this ground screen, a very complicated calculation for metering the focussing distance would be needed, involving the exact knowledge of the geometrical-optical data of the camera

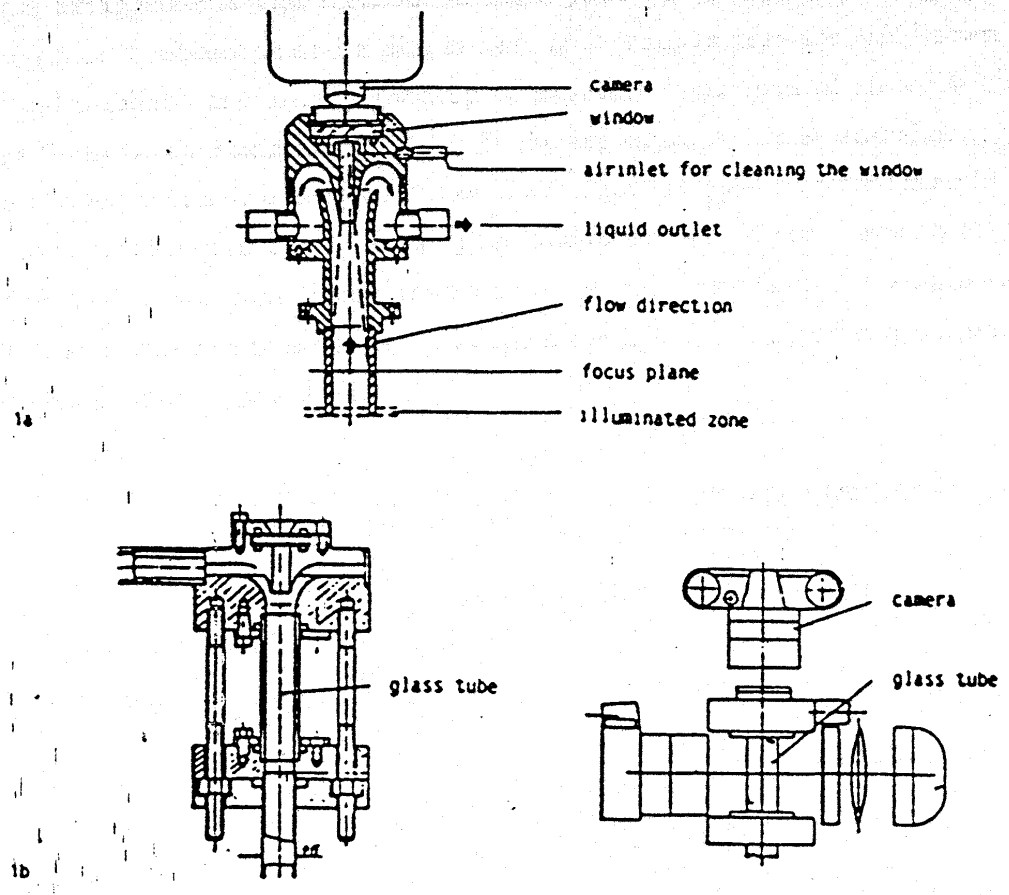

Fig. 1: Optical arrangement for axial measurements in two-phase flow

Fig. 2: Photograph of flow pattern in two-phase flow

and its lenses. Telelenses of long focussing distance show great advantages because they are forming an image with clear and well defined outlines within only a very narrow range.

3. Highspeed cinematography

The usual arrangements and methods of high-speed cinematography using a high frequency flash or stroboscope and a film camera or a drum-camera are well known. These devices and methods are usually good up to exposure frequences of 10 to 20 kHz with exposure times of approximately $10^{-6}s$. If shorter exposure times and shorter periods between two exposures are needed, a special arrangement called Cranz-Schardin-camera can be used, as shown in Fig.3. This device allows exposure times down to $10^{-8}s$ with intervals between two exposures variable from several seconds to some micro-seconds. However, the number of pictures taken in one series is limited, depending on the number of electrodes producing the flashes.

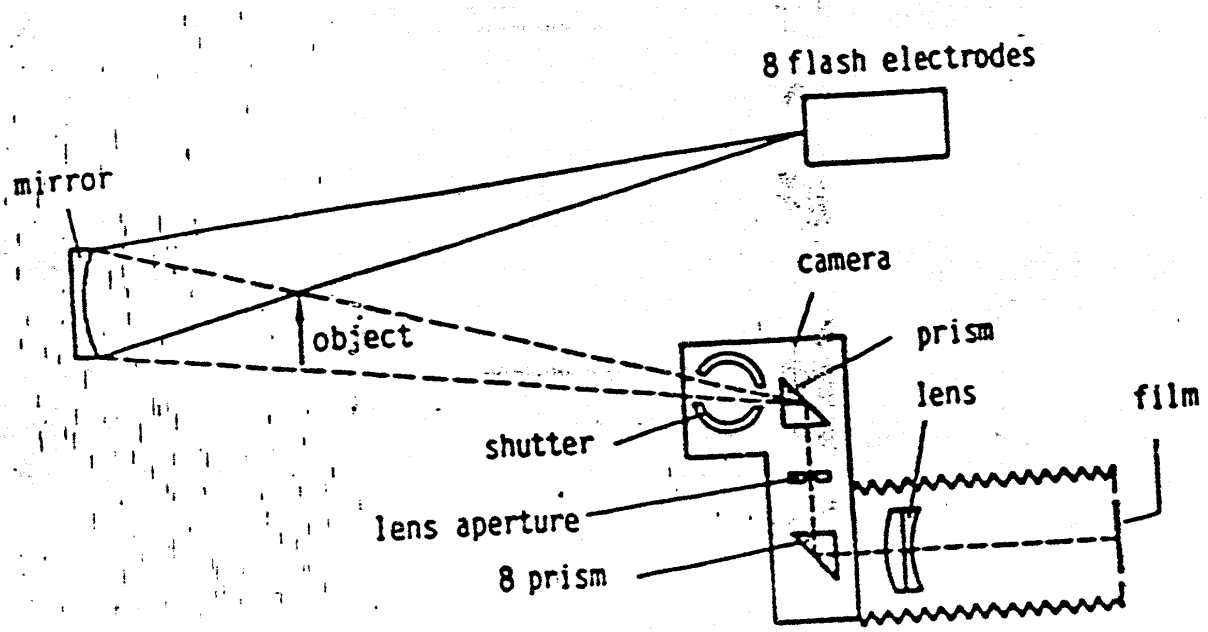

Fig. 3: Cranz-Schardin-camera for ultra short-time cinematography

The electrodes are ignited in the desired intervals and each flash is producing an image via the parabolic or spheric mirror and a prism. The electrodes are arranged in one plane, however. displaced horizontally and vertically. Due to this arrangement also the pictures produced by the series of flashes are displaced and all pictures can be registered on one photographic plate. The shutter of this Cranz-Schardin-camera is open until all flashes are ignited. By this method it is possible to register even very tiny particles flowing with an extremely high velocity, as Fig.4 demonstrates. The photograph in Fig.4 shows two exposures taken in a time distance of $10^{-5}s$ of a small liquid membrane in the nozzle of a venturi-scrubber flowing with a velocity of 80 m/s. From the two exposures registered on one photographic plate not only the velocity and its direction but also the deformation

Fig. 4: Double-exposure photograph of a liquid membrane in a Venturi-scrubber /3/

of the membrane can be easily and exactly evaluated.

The optical methods discussed up to now allow to improve the comprehension of the phenomenology of gas-liquid-flow and also to evaluate the velocity and its direction. In many cases, however, the flow of gas-liquid- or vapour-liquid-mixtures is affected by the heat transfer. In these cases also the temperature distribution near the heated wall or near the phase interface are of interest. In single-phase flow optical interference methods for registering the temperature fields in fluids are in use since a long time, as for example the Mach-Zehnder-interferometer. All these methods, however, demand a so-called comparison-object in which all fluiddynamic phenomena are identical with that in the test area, with the only exception that the comparison-object is not affected by heat transport. For vapour-liquid-mixtures such comparison conditions being exactly in phase with the process in the tested area cannot be produced or verified. Therefore, another method - the so-called holographic interferometry - is used.

4. High-Speed Holography

In 1949 Gabor /4/ invented a new optical recording technique which he called "holography". In contrast to photography by which only the two-dimensional irradiance distribution of an object is recorded, holography allows the recording and reconstruction not only of the amplitude but also of the phase distribution of the wave-fronts. Making use of this unique property, completely new interference methods could be developed. As

holography demands a highly coherent light source it can be only performed by using a laser.

The general theory of holography is very comprehensive and for a detailed description one must refer to the literature /5-7/. Here only the principals necessary for understanding the holographic measurement techniques can be mentioned. In Fig. 5 the holographic two-step image-forming process of recording and reconstructing of an arbitrary wave-front is illustrated.

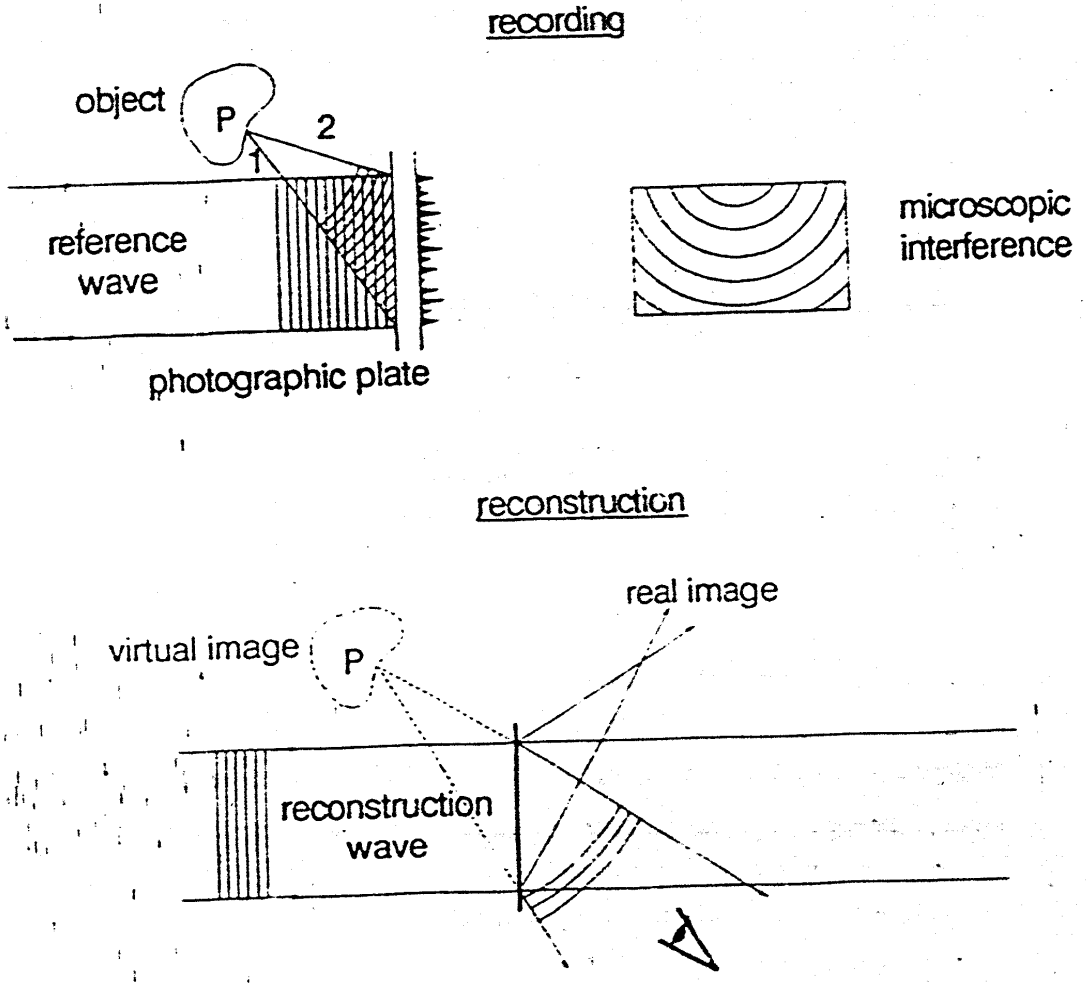

Fig. 5: Holographic two-step image forming process

The object is illuminated by a monochromatic light source and the reflected, scattered light falls directly onto a photographic plate. This object wave usually has a very complicated wave-front. According to the principal of Huygens one can, however, regard it to be the superposition of many elementory spherical waves. In order to simplify the matter, only one wave is drawn in Fig. 5. This wave is superimposed by a second one

called "reference wave". If both waves are mutually coherent they will form a stable interference pattern when they meet on the photographic plate. This system of fringes can be recorded on the photographic emulsion. After the chemical processing of the plate -in a developing bath and in a fixer-, it is called "hologram". The amplitude is recorded in the form of different contrast of the fringes and the phase in the spatial variations of the pattern.

If the plate is subsequently illuminated by a light beam similar to the original reference wave the microscopic pattern acts like a diffraction grating with variable grating constant. The light transmitted consists of a zero-order wave, travelling in the direction of the reconstructing beam plus two first-order waves. One of these first-order waves travels in the same direction as the original object wave and has the same amplitude and phase-distribution. Thus a virtual image is obtained. The other wave goes in the opposite direction and creates a real image of the object. The virtual image can be looked at with the naked eye and the real image can be studied with reconstruction devices for example with a microscope.

This holographic technique can be used instead of the photography for example for recording a swarm of droplets produced in an injection nozzle. The holograhic set-up for such a study is shown in Fig. 6.

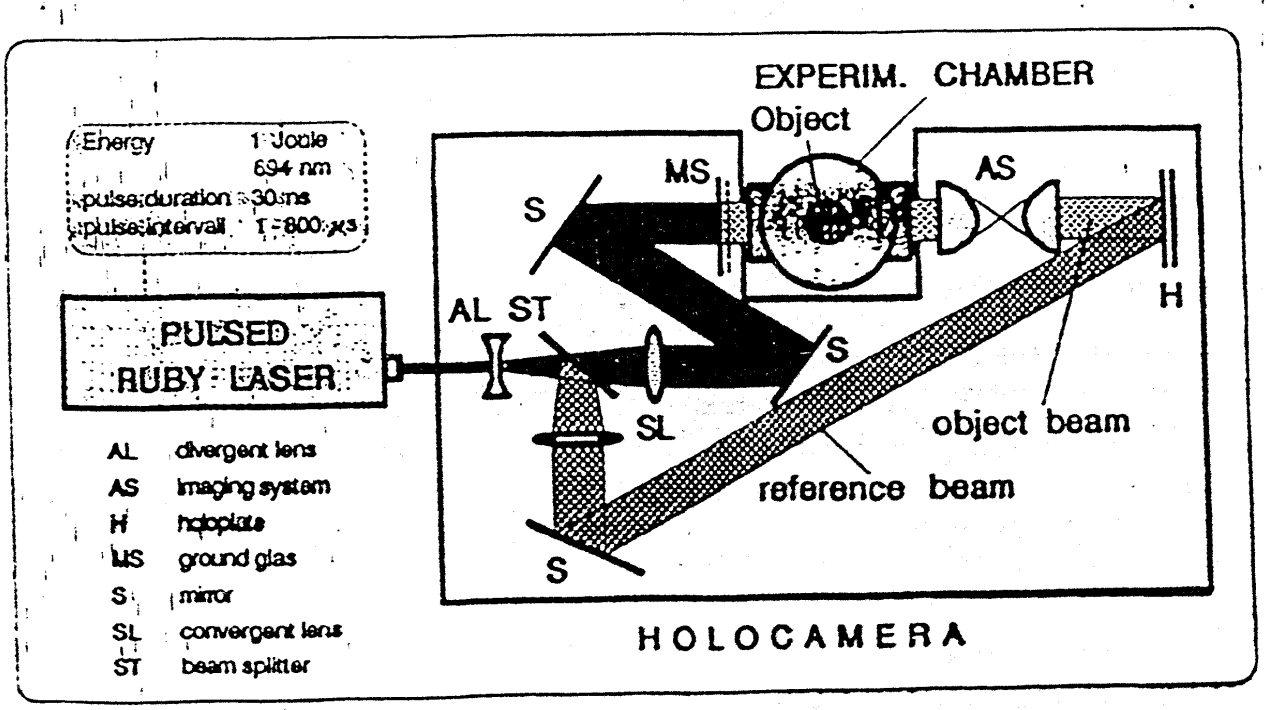

Fig. 6: Optical arrangement for the recording of pulsed laser holograms

It consists of a pulsed ruby laser emitting pulses of a period of 30 ns and a lens- and

mirror-system for expanding, dividing and guiding the laser beam through the measuring object and onto the holographic plate. The laser beam is first expanded by means of the lens AL and then divided in the beam splitter ST to produce the object beam and the reference beam. The object beam travels via a collecting lens, two mirrors and a screen through the object - in this case the spray coming out of a nozzle - and passes after the object an imaging lens before it falls onto the holographic plate. There it is superimposed by the reference wave which is splitted off by the beam splitter ST and falls via the collecting lens SL and a mirror onto the photographic plate by-passing the object. So an instantaneous picture of the situation in the spray can be registered. If the electronic system of the ruby laser allows to emit more than one laser pulse within a very short period of time sequences of the spray behaviour can be stored on the photographic plate from which the velocity of the droplets with respect to amount and direction as well as changes in the size and geometrical form of the droplets can be evaluated. This evaluation, however, needs a very sophisticated and computerised procedure.

For evaluating the hologram it first has to be reconstructed as demonstrated in Fig. 7.

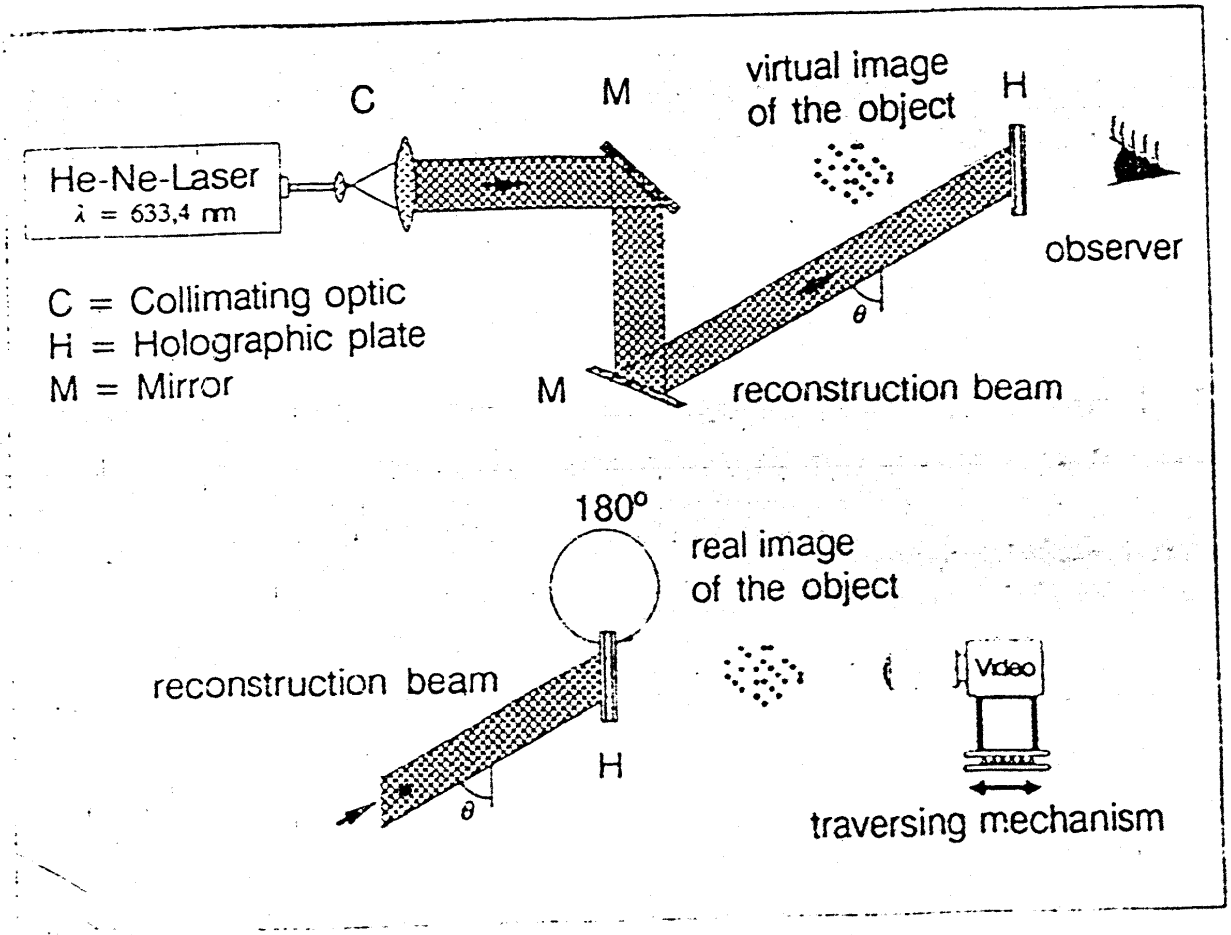

Fig. 7: Optical arrangement for the reconstruction of pulsed laser holograms

To do this for the special application of studying a nozzle spray, the holographic plate is replaced to the old position after chemical processing and is now illuminated by a continuously light emitting helium-neon-laser, sending its light via the path of the reference beam described in Fig. 6. This new beam is now called reconstruction beam. If the holographic plate is replaced in the same orientation as it stood when the exposure occurred one can look at it with the naked eyes and can see a virtual image of the droplet spray exactly at the place where it was produced before by the injecting nozzle. For a quantitative evaluation one needs a closer examination by a camera, for example by a video camera. To do this the holographic plate has to be turned by 180°, when positioning to the old place and by illuminating with reconstruction beam a real image of the spray is produced, however, on the other side of the holographic plate. This real image has a three-dimensional extension and the video camera can be focussed to any plane within the image. For technical evaluation the camera, fixed at a certain position, is focussed to the mid-plane and then for getting information from other planes of the spray the camera is moved forward or backward with fixed focus of the lens. So plane by plane of the spray cloud can be evaluated. The virtual picture one would see with the naked eye is demonstrated in Fig. 8.

It looks like a photographic picture of a spray with a veil near the nozzle orifice and a swarm of droplets separating from this veil when it breaks up. The quantitative evaluation works via the above-mentioned video camera and a computer system as shown in Fig. 9 and uses the real picture. Main components of this evaluating systems are a digitiser, a graphic monitor, a video camera and a PC. The video camera is scanning the real image of the reconstructed hologram O and sends its information to the digitiser D. It changes the electrical signal from a analogue character to a digital one and stores it in a frame memory. Now the computer C can use the digitalised information for performing the image reprocessing. The digitiser simultaneously produces an analogue picture in a false-colour (red-green-blue) reproduction.

The procedure going on in the computer is briefly outlined in Fig. 10. After a first positioning of the camera, noise-signals are eliminated without suppressing the gradients of the grey-colour. By this a first "clean" picture (with a minimum of noisy signals) is arising. Then the rest of pixels still originating from noisy signals is filtered out.

In the next step gradients out of the less or more intensive grey-colours of the pixels surrounding the holographic reproduction of the droplets or of the contour of the veil are evaluated. So it can be distinguished between well focused parts and such ones which are out of focus. Then all pixels having a grey-colour below a certain pre-defined value are treated as zero. By this reproductions of droplets which are out of the interesting

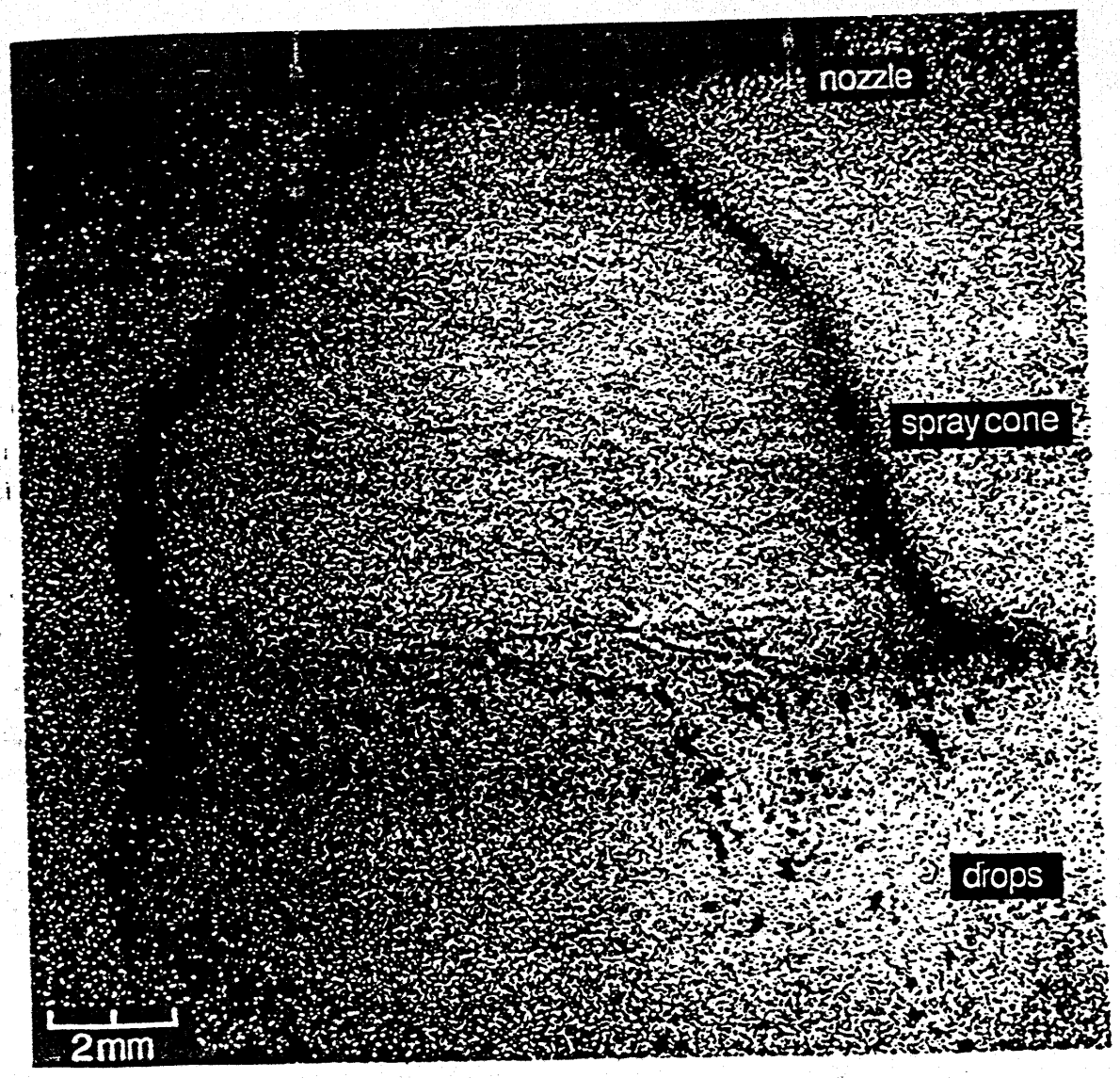

Fig. 8: Photography of a reconstruction of a pulsed laser hologram.
Object: Spray of a hollowed cone spiral nozzle.

focus-plane can be eliminated and a "picture" is electronically produced containing only reproductions of droplets which were within a very narrow tolerance within the focussing plan of interest.

By this procedure it happens that the contours of some droplets do not have a closed and continuous outline, because pixels may have been extinguished spotwise during the gradient checking procedure. Therefore a next step follows in which the open contours are filled with colour to produce closed outlines of the droplet reproductions. To be sure not erroneously to create new spots by this process which could be interpreted as droplet reproductions, the situation after the contouring is compared with that which existed before reproductions of droplets out of focus were eliminated. A "droplet" in

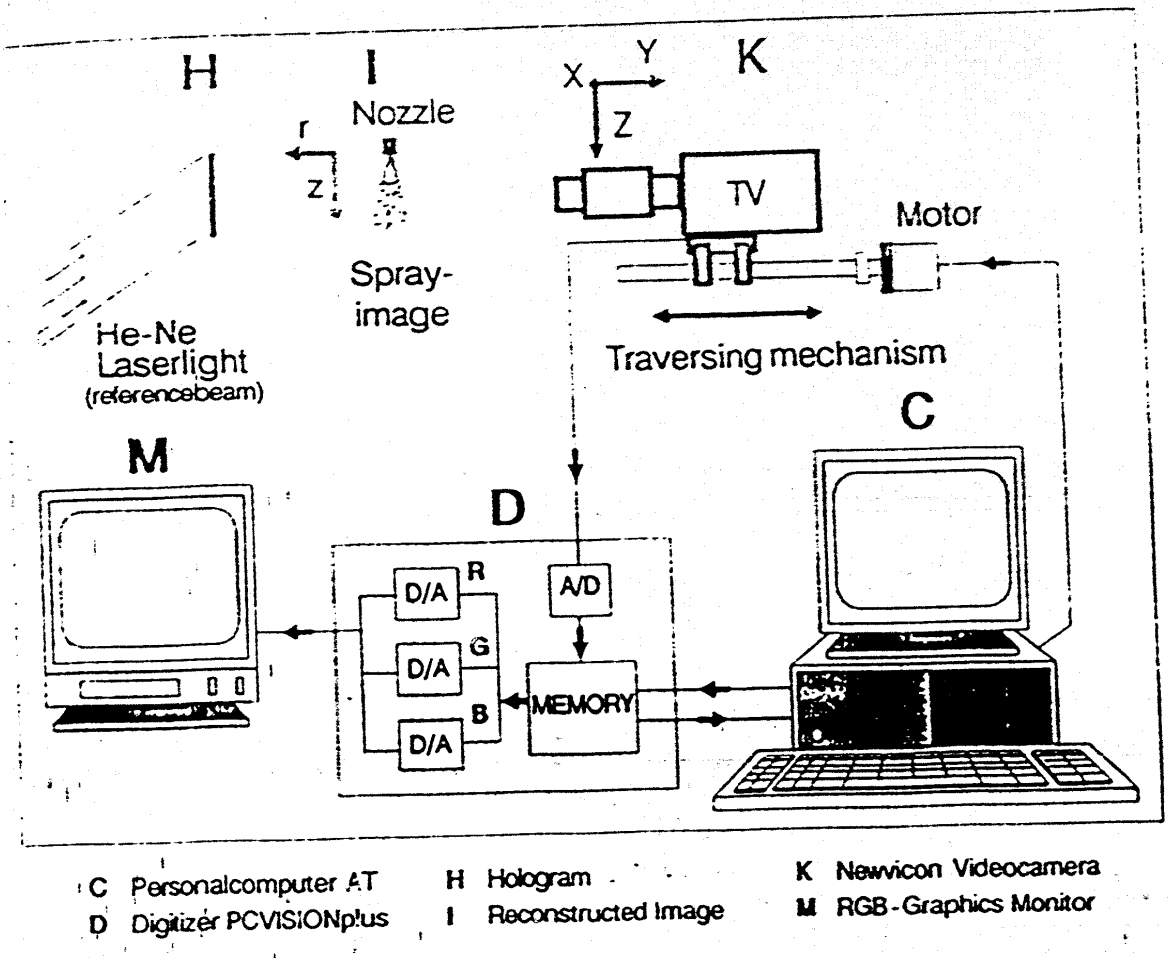

Fig. 9: Digital image processing system for the evaluation of pulsed laser holograms

the new picture is only accepted if it existed already before in the old picture. Finally the remaining droplet-reproductions are filled with colour and now the evaluation with respect to droplet-size, -form and -concentration can go on.

After this plane in the holographic picture has been evaluated the video-camera is moved within a small step and the whole procedure starts again. So plane by plane of a spray-cloud can be evaluated and a three-dimensional picture of the two-phase flow situation is arising which was fixed on the holographic plate within a few nanoseconds. For more detailed information reference is made to the work by Chávez and Mayinger /8, 9/.

More downstream of the nozzle only droplet clouds can be observed. By evaluating a great number of such droplet clouds with the above-mentioned procedure information can be extracted with respect to the dependency of the droplet diameter from the mass-flow-rate through the nozzle and the pressure of the atmosphere into which the spray is injected. An example of such an evaluation gives Fig. 11.

If two exposures of a droplet spray are illuminated onto the same holographic plate within

Fig. 10: Evaluation of a single pulsed hologram

a short period of time also the velocity of the droplets can be determined from such an hologram, however, with a much more complicated procedure which is described in detail in /9/. The data produced by this opto-electronic process are of high accuracy as Fig. 12 demonstrates. Especially the suspicion that the computerised processing of the double exposure hologram produces a large scattering in the velocity-data is misproved by this figure. Even the influence of the pressure of the atmosphere in which the droplets are travelling is clearly brought out.

If the droplets are moving in a vapour atmosphere of the same substance as the liquid and if the temperature of the liquid is below the saturation temperature condensation occurs at the phase-interface which makes the volume of the droplet growing. By using a simple energy balance the condensation heat transfer can be calculated from this growth of volume versus time. The accuracy and the reproducibility of the described opto-electronic measuring technique are good enough to determine these heat transfer coefficients at the veil and at the droplet-cloud as Fig. 13 demonstrates. The heat transfer data are averaged values from all droplets, being reproduced in a hologram.

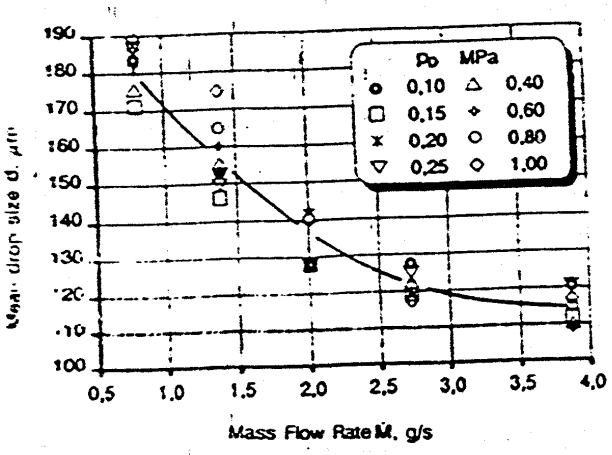

Fig. 11: Mean droplet diameter as a function of the mass flow rate at different ambient pressures

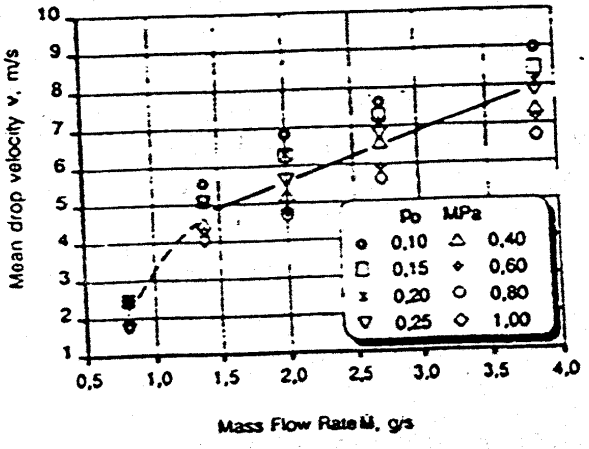

Fig. 12: Mean droplet velocity as a function of the mass flow rate at different ambient pressures

5. Holographic Interferometry

For convective heat transfer processes the temperature gradient in the boundary layer near the heat emitting or absorbing wall is of special interest because from the temperature gradient at the wall, supposing a laminar sublayer the heat transfer coefficient

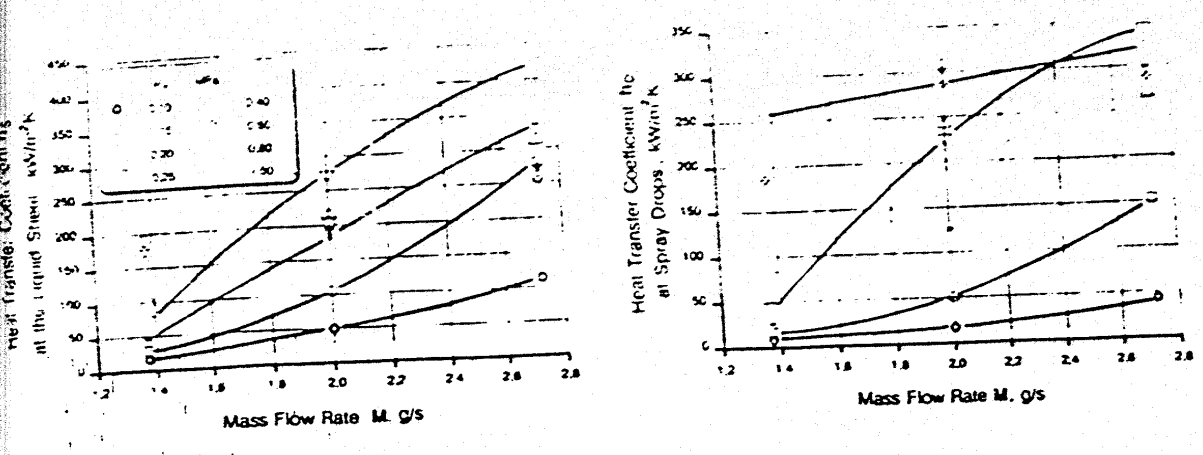

Fig. 13: Heat transfer coefficient at the liquid sheet and at the droplets as a function of the mass flow rate at different vapor pressures

$$h = \frac{-k\left(\frac{dT}{dy}\right)_w}{T_w - T_\infty} \tag{1}$$

can be directly derived if, in addition, the temperature of the wall or of the bulk and the thermal conductivity of the fluid are known. This temperature gradient can be measured by interferometric optical methods, like the Mach-Zehnder interferometry, as well-known from the literature.

A new interferometry method is the combination of holography and interferometry. A most commonly used arrangement of optical set-ups for this holographic interferometry is shown in Fig. 14.

A helium-neon-laser or an argon-laser serves as a light source emitting continuously monogramatic and coherent light. By means of a beam splitter the laser beam is divided into an object- and a reference-beam in a similar way as we learnt before. Both beams are then expanded to parallel waves by a telescope which consists of a microscope objective and a collimating lens. The object-wave passes through the test section in which the temperature is to be examined whereas the reference-wave directly falls onto the photographic plate. There are many possibilities for arranging the optical set-ups to form a holographic interferometer which cannot be discussed here in detail. Reference is, therefore, made to the literature for example /10, 11/.

Several procedures exist to produce interferograms; here only a sophisticated one will be explained, which can be used for high-speed cinematography and by which transient heat transfer phenomena can be examined. It is called "real-time-method" because it

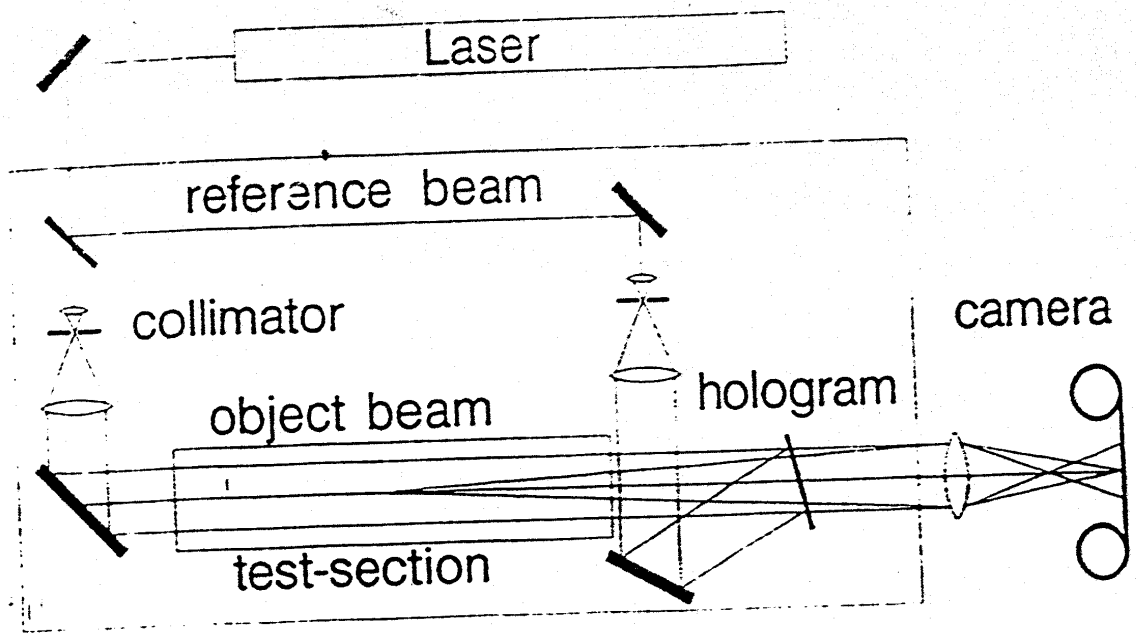

Fig. 14: Optical set-up for holographic interferometry

allows to observe a process to be investigated continuously in real time. The method is illustrated in Fig. 15.

After the first exposure, by which the comparison-wave is recorded and during which there is no heat transfer in the test section –for two-phase flow experiments, even only single- phase flow may exist– the hologram is developed and fixed. Remaining at its place or repositioned accurately, the comparison-wave is reconstructed continuously by illuminating the hologram with the reference-wave. This reconstructed wave can now be superposed onto the momentary object-wave. If the object-wave is not changed and the hologram is precisely repositioned, no interference fringes will be seen at first (infinite-fringe-field adjustment).

Now the heat transfer process which is to be examined and for two-phase flow for example the boiling with bubble formation, or the condensation can be started. Due to the heat transport process a temperature field is formed in the fluid and the object-wave receives an additional phase shift passing through this temperature field. Behind the hologram both waves interfere with each other and the changes of the interference pattern can be continuously observed or photographed on still or moving film.

The real-time-method demands an accurate reconstruction of the comparison-wave; therefore, the hologram must be repositioned precisely at its original place. This can be done by using a well-adjustable plate-holder, which, nowadays, can be purchased from the market. It is recommended to use a plate-holder where the final adjustment can be done via

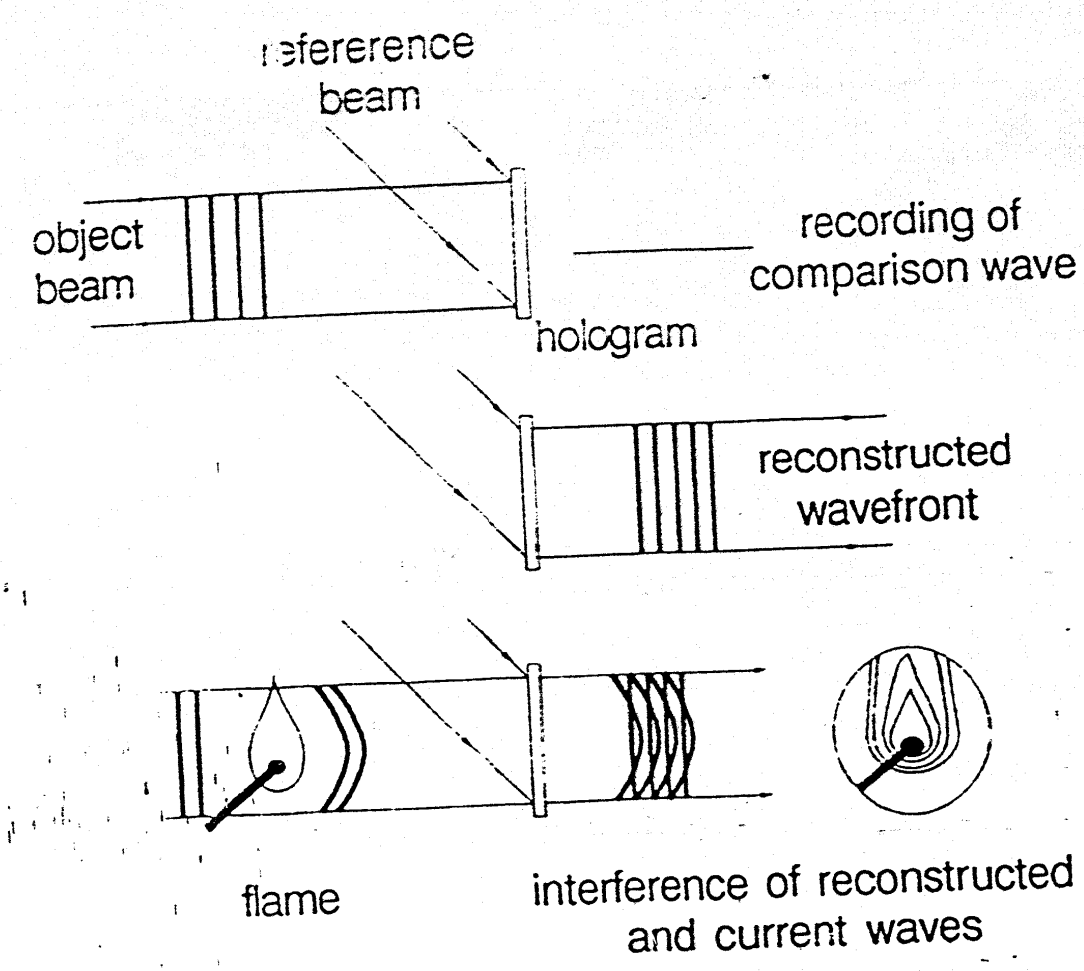

Fig. 15: Real time method for holographic interferometry

a remote control for example with quartz crystals. The adjustment of the repositioned holographic plate gets its feed-back control signals on an optical basis because the adjustment has to be done in such a way that the interference fringes –at first visible due to non-precise position of the plate– disappear during this procedure. This, certainly, has to be done without the heat transfer process having started, however, the pressure and the temperature are existing under which the system is operated during the experiments.

A series of holographic interferograms taken with this method is illustrated in Fig. 16, where the bubble formation at a heated surface in water with slow horizontal flow was studied. The water is slightly subcooled, i.e. the bulk temperature of the water was below the saturation temperature and, therefore, the bubble is condensing again after detaching from the heated surface and departing from the superheated boundary layer as one can observe by following the holographic interferograms versus a period of 7 ms in Fig. 16. The horizontal black and white fringes in Fig. 16 represent lines of constant temperature in a first approximation.

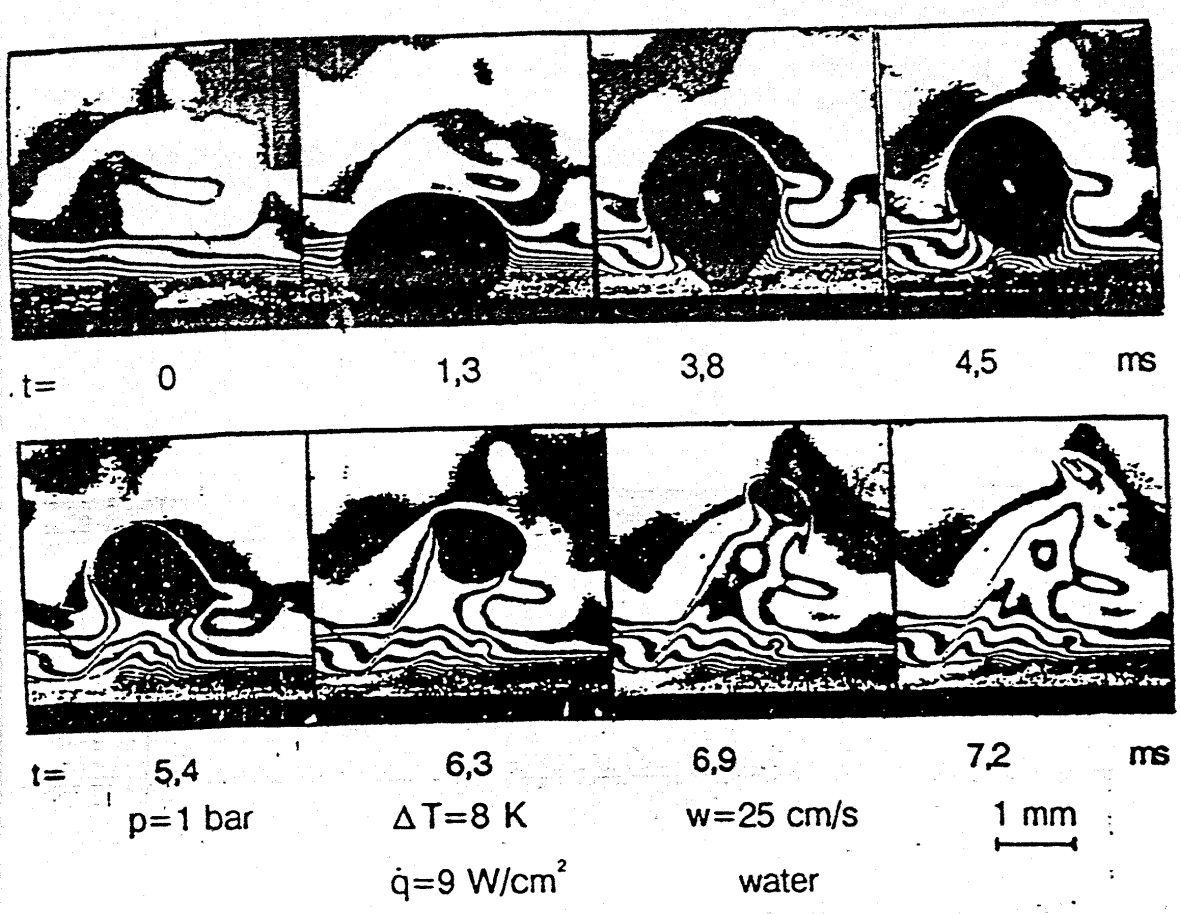

Fig. 16: Interferogram of subcooled boiling on a heated wall

From this figure, however, we can also learn something about the limitation with which this and all other interferometric methods are afflicted. The temperature field near the heated wall in the fluid is not only shifting the phase of the light-wave, it is also deflecting the light beam when travelling through it. This deflection has the consequence that with very high gradients at the wall –as it is the case in subcooled boiling– the zone immediately adjacent to the wall cannot be seen. With lower heat fluxes this deflection is not a problem in interferometry.

For learning the procedure of evaluating such an interferogram a more simple example shall be used as that in Fig. 16. Fig. 17 shows the interference fringes in a subchannel of a tube-shell heat exchanger formed by three heat emitting tubes. The interference fringes here represent exactly isotherms in the fluid around the tubes and it can be clearly seen that the spacing of these isotherms is differnt at positions of narrow and of wider gap-size in the subchannel. Wide-spreading of the isotherms means a low temperature gradient and as we know from experience a low heat transfer coefficient.

The temperature field in the subchannel is of two-dimensional nature with good approximation. For the sake of simplicity only the evaluation of the simple case of a

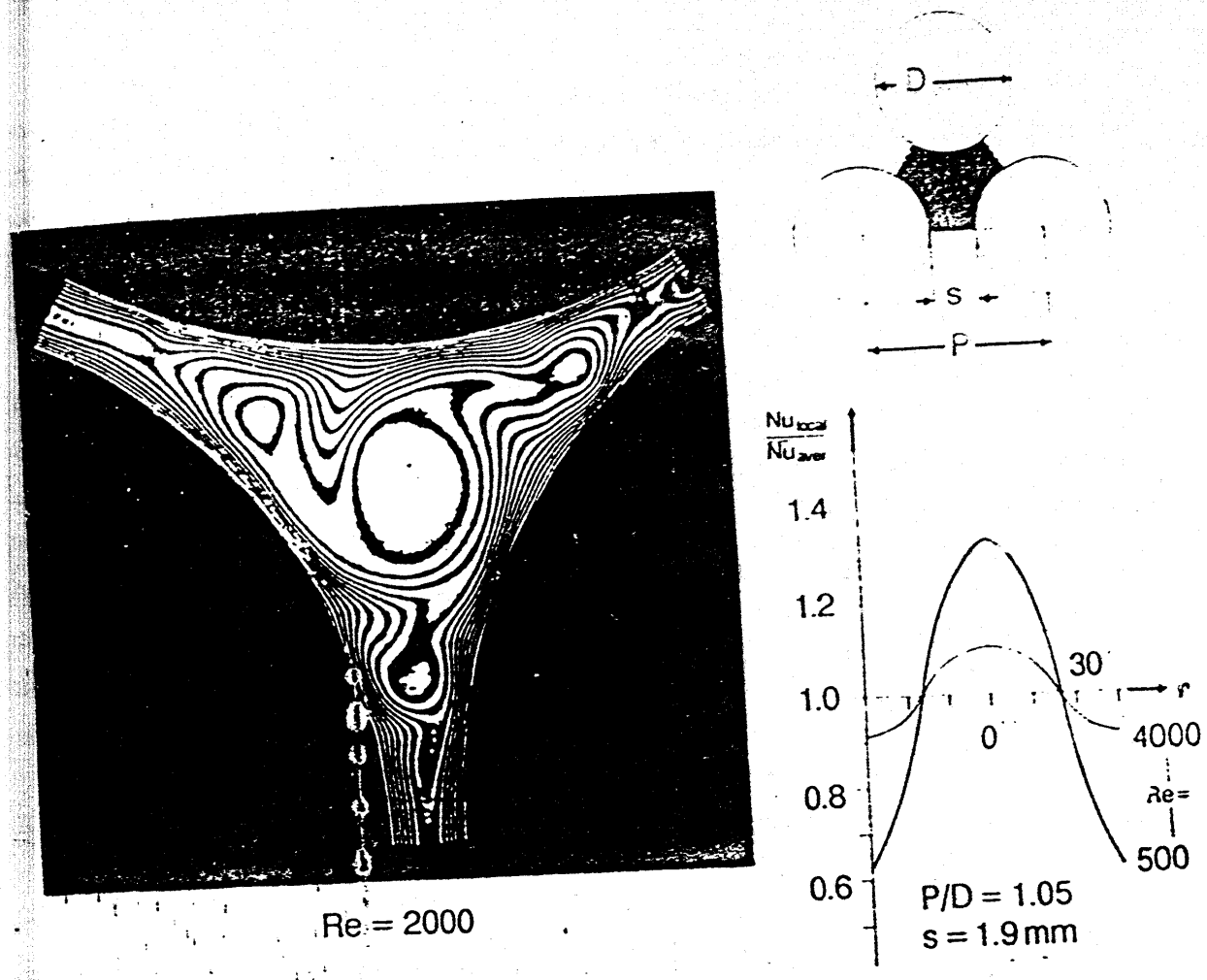

Fig. 17: Temperature field between three heated tubes with coaxial flow

two-dimensional temperature field will be discussed here. It is also assumed that the holographic interferogram is produced with parallel object-waves. The evaluation of the interference patterns is than quite similar to that of a Mach-Zehnder-interferometer /11/. Therefore, here only the basic equations will be given. In the holographic interferometry the object-waves passing through the test section at different time are superposed and, therefore, reveal the changes in optical path-length between the two exposures. Expressed in multiples S of a wave-length λ, this change is calculated to

$$S(x,y)\,\lambda \;=\; l\,[\,n(x,y)_2 \;-\; n(x,y)_1\,] \qquad (2)$$

where l is the length of the test section in which the refractive index n is varied because of temperature changes. The refractive index distribution $n(x,y)$ during the recording of the two waves is -as mentioned above- assumed to be two-dimensional (no variation in light direction). Equation (2) shows that initially only local variations can be determined. Only if the distribution of the refractive index $n(x,y)_1$ during the recording of the comparison

wave is known, absolute values can be obtained. Therefore, one usually establishes a constant refractive index field (constant temperature) while recording the comparison wave.

$$S(x,y)\,\lambda \;=\; l\,[\,n(x,y)_2 \;-\; n_\infty\,] \tag{3}$$

To obtain absolute values for the temperature field, the temperature at one point in the fluid has to be determined by thermocouple measurements. This is usually done in the undisturbed region or at the wall of the test chamber. Equ. (3) is the equation of ideal interferometry. It is assumed that the light beam propagates in a straight line. Passing through a boundary layer, the light beams, however, are deflected because of refractive index gradients. This deflection is used for the various Schlieren- and shadowgraph-methods. The light deflection can be converted into an additional phase shift S, if a linear distribution of the refractive index is assumed to be within this small area.

$$\Delta S \;=\; \frac{n_0\,\lambda\,l}{12\,b^2} \tag{4}$$

In this equation b is the fringe width and n_0 is the average refractive index.
In many applications an ideal, two-dimensional field cannot be found. Often the boundary layer extends over the ends of the heated wall, or there are entrance effects or temperature variations along the path of the light beam (axial flow in the test section). Therefore, only integrate values are obtained. Having corrected the interferogram, the obtained refractive index field can be converted into a density field The relation is given by the Lorentz-Lorenz-formula where N is the molar refractivity and M the molecular mass.

$$\frac{n^2-1}{n^2+2}\,\frac{1}{\rho} \;=\; \frac{N}{M} \tag{5}$$

If there is only one component in the test section and the pressure is kept constant, the density variations can only be caused by temperature changes. If the fluid is a gas, the situation is very simple because its refractive index is very near to 1, which reduces Equ. (5) to the Gladstone-Dale equation:

$$\frac{2}{3}(n-1)\,\frac{1}{\rho} \;=\; \frac{N}{M} \tag{6}$$

With the simple Boyle-Mariotte law and R as the gas constant we then obtain the following formula, which relates the fringe shift to the temperature:

$$T(x,y) = \left[\frac{S(x,y)\, 2\, \lambda\, R}{3\, N\, p\, l} + \frac{1}{T_\infty} \right]^{-1} \qquad (7)$$

For liquids the procedure is a little more complicated because we have to take in account the real behaviour of the thermodynamic properties as a function of temperature. Therefore, we have to use an equation of state for the refractive index n or we have to take the refractive index from tables interpolating the data with simple equations. Fortunately, there are good data banks available in the literature for most of the fluids. However, it is also not difficult to measure the refractive index in a simple optical set-up.
With an equation for the refractive index as function of the temperature we then can use Equ. (2) and we get the connection between the pattern of the interference fringes and the temperature field, as shown in Equ. (8):

$$S(x,y)\, \lambda = \frac{dn}{dT} \left[T(x,y) - T_0 \right] \qquad (8)$$

Often local heat transfer coefficients are of special interest. In this case the temperature gradient at the wall is determined and assuming a laminar boundary layer next to the wall or the phase-interface the heat transfer coefficient is obtained by using Equ. (1).
The assumption that the temperature field is two-dimensional and constant along the path of the beam traveling through the fluid is not valid in case of temperature fields around curved surfaces, like bubbles. The refractive index n is then a function of the radius r, and we have to use Equ. (2) in its differential form

$$S\, \lambda = \int_0^1 (n - n_0)\, dz \qquad (9)$$

and we write it in spherical or cylindrical co-ordinates:

$$S(y)\, \lambda = \int_0^x \left[n(r) - n_0 \right] dz \qquad (10)$$

For spherical and cylindrical symmetry Equ. (10) can be solved and integrated as described, for example, in /15/ after transforming it in the form

$$S(y)\, \lambda = 2 \sum_{k=i}^{N-1} \Delta\, n_k \left[\left(r_{k+1}^2 - r_i^2 \right)^{1/2} - \left(r_k^2 - r_i^2 \right)^{1/2} \right] \qquad (11)$$

In temperature fields with very high gradients the deflection of the laser beam, which is demonstrated in Fig. 18, too, cannot be neglected, as it is done in the evaluating

procedure described in /13/. High temperature gradients are especially found in the liquid boundary layer around vapour bubbles, in particular if condensation occurs. In such a case a complicated correction procedure for this deflection has to be used which is described by Nordmann and Mayinger /14/ and by Chen /15/. With the equations and corrections described there, even temperature fields around very tiny bubbles can be evaluated.

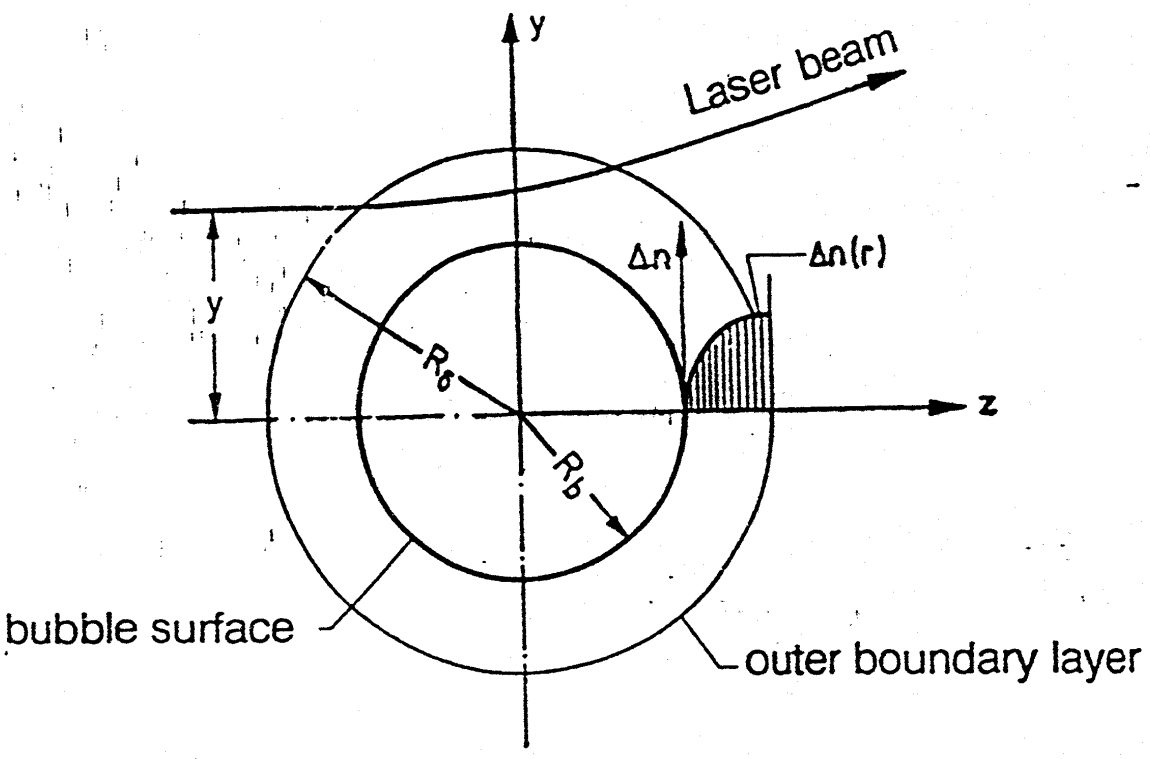

Fig. 18: Beam deflection and optical conditions in a temperature field around a spherical bubble

With high heat transfer coefficients the boundary layers at the phase-interface are usually very thin –in the order of a few hundredth of a millimeter– and it is difficult to investigate them with the interferometric procedure described up to now, because only a few interference fringes would be observed within this narrow area. Therefore, here another interference method has to be used, the so-called "finite fringe method". In this method, after the reference hologram was produced, a pattern of parallel interference fringes is created by tilting the mirror in the reference-wave of Fig. 19, or by moving the hologram there within a few wave-lengths. The direction of the pattern can be selected as one likes and it is only depending on the direction of the movement of the mirror or of the holographic plate.

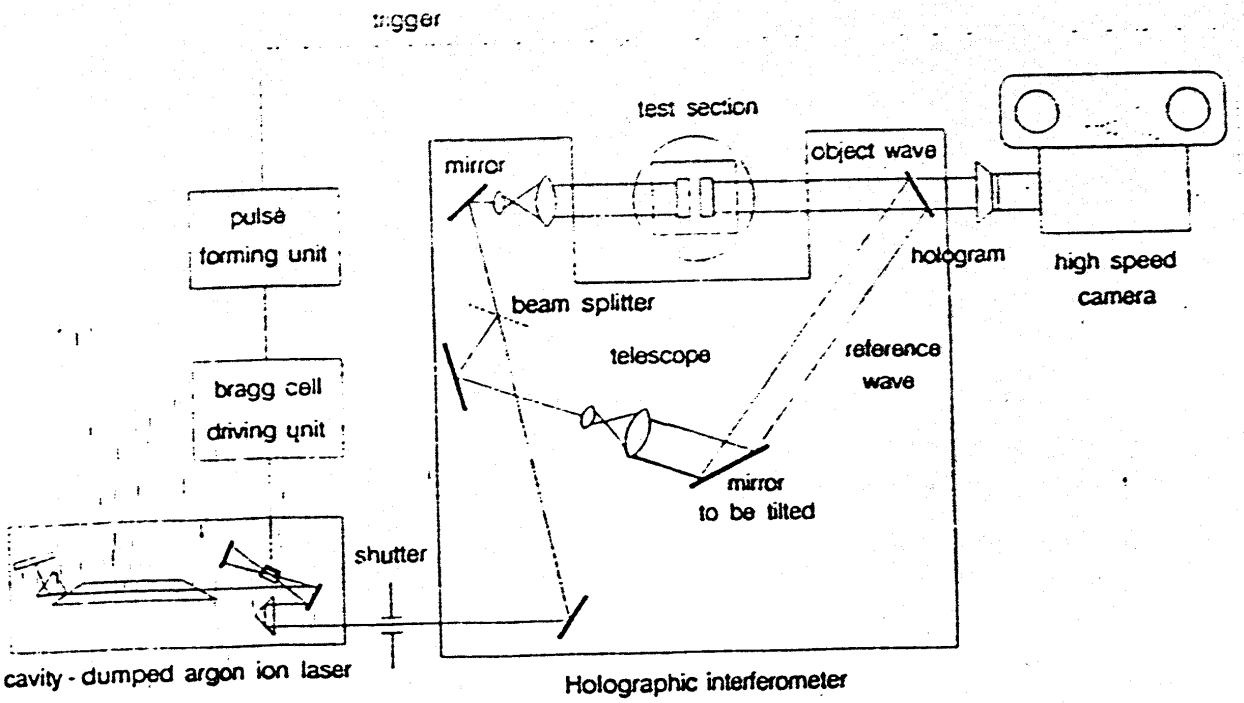

Fig. 19: Arrangement for holographic interferometry with finite fringe method

This pattern of parallel interference fringes is then distorted by the temperature field due to the heat transfer process. The distortion or deflection of each fringe from its original -parallel- direction is, in a first rough approximation, the temperature gradient and gives by using Equ.(1) the heat transfer coefficient. A short description how these interference patterns are evaluated is given in Fig. 20. This figure also demonstrates for the example of a temperature field around a burning flame how these distorted interference fringes look like, depending on the original orientation of the parallel pattern. A detailed description of the mathematical procedure how to evaluate these pattern of finite fringes and how to determine the temperature gradients from it, is given in (11) and (12).

Fig. 21 demonstrates the possibilities of using these techniques in a flow with a bubble condensing in a liquid. By combining this method with the high-speed cinematography it allows an inertialess and precise evaluation of the heat transfer coefficient at the phase-interface of a condensing bubble. Holographic interferometry certainly can only be used if the flow situation is not too complicated and if the bubble population is not too numerous, so that individual bubbles can be identified. It is not possible to look inside the bubbles, because the light is totally reflected at the phase-interface.

As explained in the Equs. 2 - 5 the phase shift is a function of the change in the density of the fluid. In pure substances the density is a function of temperature and pressure. In multi-component systems also the concentration influences the density. In our evaluation

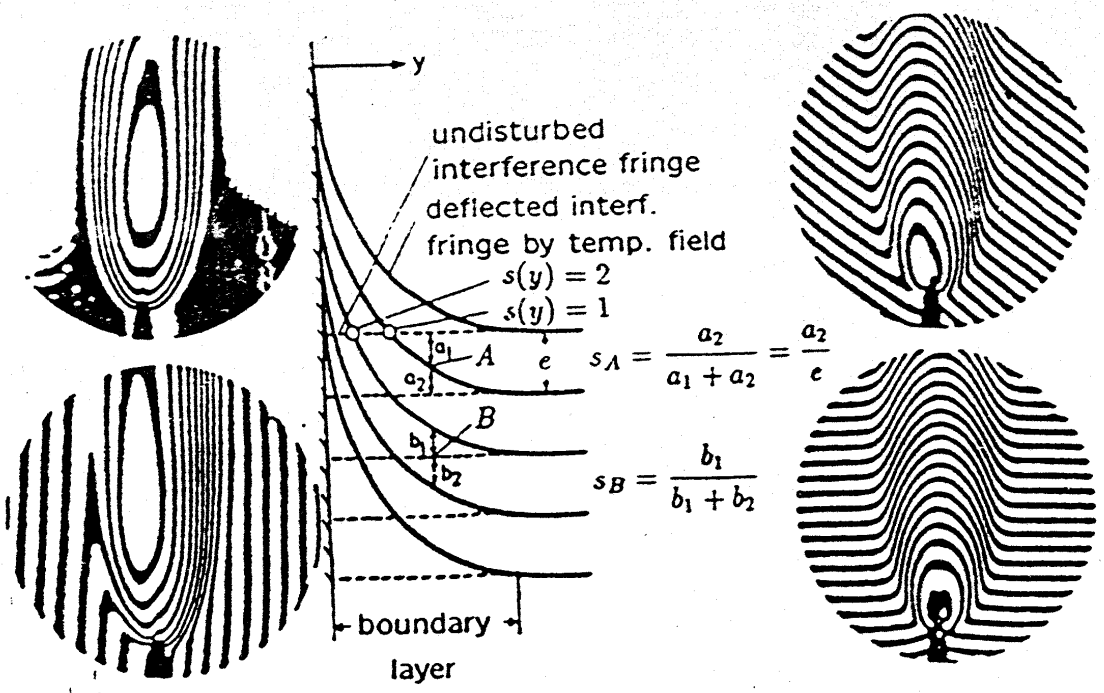

$$s_A = \frac{a_2}{a_1 + a_2} = \frac{a_2}{e}$$

$$s_B = \frac{b_1}{b_1 + b_2}$$

Fig. 20: Finite fringe interferograms (temperature field around a flame) and their evaluation

procedures up to now we worked on the assumption that the alteration of the density is affected by a temperature change only and, therefore, the variations in the refractive index within the test section could be treated as temperature distributions. When the variations in the refractive index are caused not only by a temperature-, but also by a concentration- or pressure-change these simple evaluation of the interference pattern, described up to now is not possible any more. Therefore, coupled heat and mass transfer processes can be examined by interferometric methods only if one of the two fields is obtained by an additional measuring method. Only by assuming identical profiles of the temperature and of the concentration the interferograms can be evaluated without additional measurements as El-Wakil /16/ did.

There is, however, one method to determine the temperature and the concentration field by optical means alone, which is called the "two-wave lengths interferometry". This is done by applying their dependence of the refractive index on the wave-length of the light to determine the temperature- and concentration-fields by means of separate interferograms, taken at different wave-lengths. Ross and El-Wakil /17/ used this two wave-lengths interferometry in a modified Mach-Zehnder-interferometer for the study of the evaporation and combustion of fuels. Panknin and Mayinger /10, 11/ used this basic

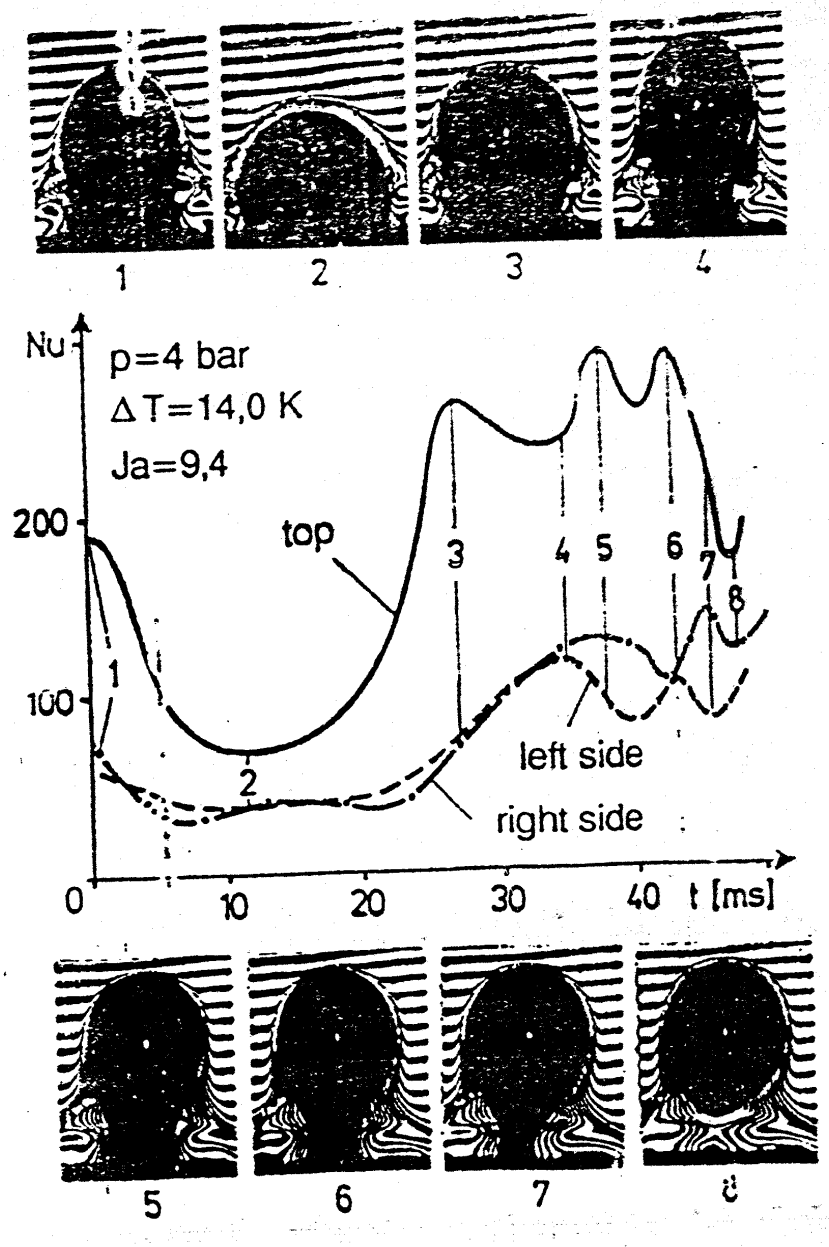

Fig. 21: High speed cinematography of interferograms around a condensing bubble and the evaluated heat transfer at the phase interface /14/

idea and developed a two-wave lengths method for the holographic interferometry. The problem with the two-wave-lengths interferometry is that the two interferograms have to be superimposed very accurately. Here, the peculiarity of the holography allowing the recording of different interference pattern on one and the same plate is a great help to overcome these difficulties. A simple set-up for the holographic two-wave lengths interferometry is shown in Fig. 22. It resembles very much the arrangement of Fig. 14 and actually the only difference is that two lasers are used as light sources in Fig. 22. The beams of the He-Ne-laser ($\lambda_1 = 6.328\text{Å}$) and of the Argon laser ($\lambda_2 = 4.579\text{Å}$) intersect

and, therefore, only one shutter is needed and equal exposure times at both wave lengths are guaranteed. The beams are then superimposed by means of a beam splitter. By this one gets two object - and two reference-waves at the different wave-lengths.

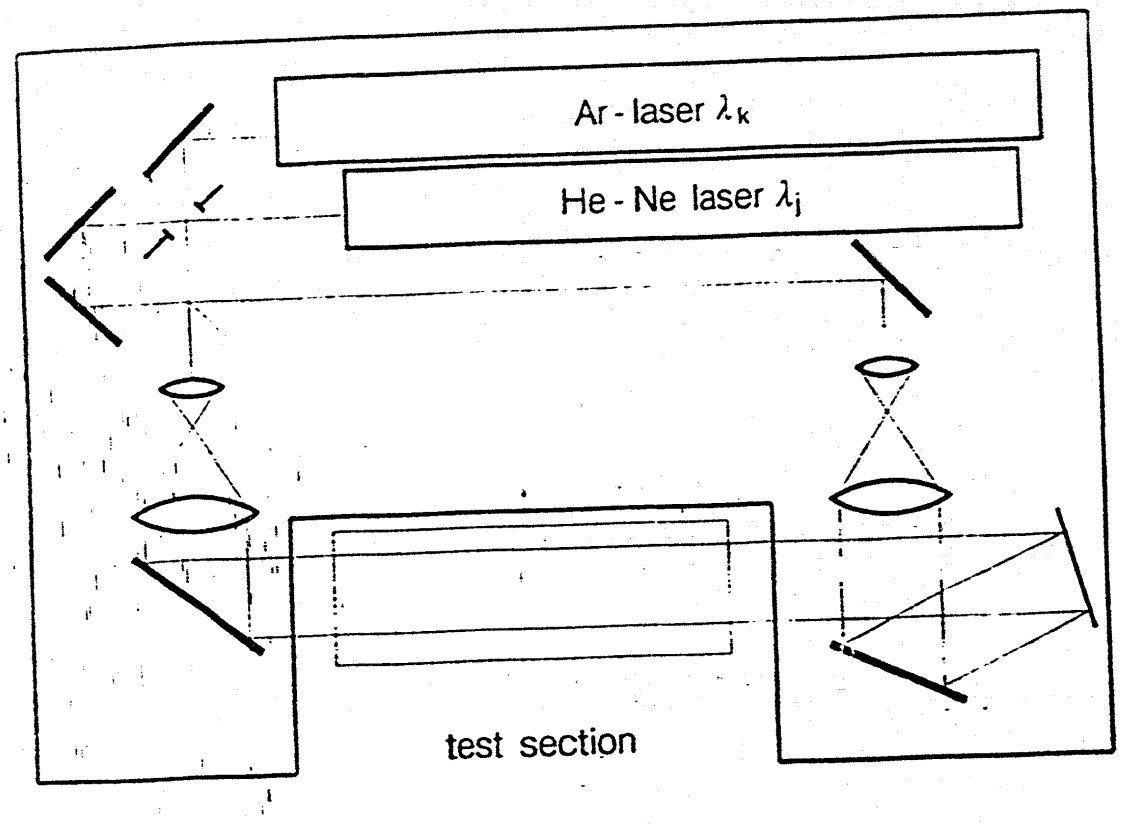

Fig. 22: Optical set-up for holographic two-wavelength interferometry

It has to be mentioned that not only the object wave λ_j is reconstructed by the reference-wave λ_j, but also a false objective-wave λ_k is obtained and vice versa. These unwanted waves, however, emerge at different angle from the hologram and can, therefore, easily be separated from the original waves. For the evaluation of the interferograms here only some simple equations shall be presented. For a more detailed study reference is made to the work by Panknin /11/. In gas we can use the Gladstone-Dale-equation, Equ. (6), and the ideal gas law which relates the fringe shift to the temperature- and concentration-distribution in a heat and mass transfer boundary layer.

$$S(x,y)\,\lambda \;=\; \frac{3\,p\,l}{2\,R}\,N_m\,\left[\frac{1}{T(x,y)} - \frac{1}{T_\infty}\right] \qquad (12)$$

The molar refractivity N_m for a mixture of two gaseous components is given by

$$N_m = N_a C_a + N_b C_b ; \qquad with \quad C_a + C_b = 1 \tag{13}$$

where N_a and N_b are the molar refractivities of the components in their pure form and C is the concentration of the component in the mixture. During the recording of the comparison wave the temperature distribution T in the test section is constant and there are only two components of the mixture.

Combining Equ. (12) and (13) we obtain for each wave-length

$$S(x,y)\,\lambda = \frac{3\,p\,l}{2\,R}\left[\frac{1}{T(x,y)}\,(N_a + C_b(x,y))\,(N_b - N_a) - \frac{N_a}{T_\infty}\right] \tag{14}$$

eliminating $C_b(x,y)$. The temperature $T(x,y)$ can be calculated:

$$S_j(x,y)\,\frac{\lambda_j}{N_{bj} - N_{aj}} - S_k(x,y)\,\frac{\lambda_k}{N_{bk} - N_{ak}} =$$

$$\frac{3\,p\,l}{2\,R}\left[\frac{1}{T(x,y)} - \frac{1}{T_\infty}\right]\left[\frac{N_{aj}}{N_{bj} - N_{aj}} - \frac{N_{ak}}{N_{bk} - N_{ak}}\right] \tag{15}$$

After determining the temperature distribution only one interferogram is used to calculate the concentration profile.

Equ. (15) shows that there is a difference between the phase shifts for the two wave-lengths which is used for the measurement of the temperature. This difference is usually very small. Therefore, the two wave-lengths used should be as far apart as possible. The dependence of $N_{(a,b)}$ is also very small and gets larger proportions only in the vicinity of an absorption line which, however, is usually not in the visible range. This limits the choice of substances to those lengths used. Some test fluids suitable for this technique are naphtalene, carbondisulphide, bencene and hexane. The position of the fringes has to be determined very accurately at the same plate in the two interferograms.

A simple application example of the two-wave-lengths technique is given in Fig. 23. In order to demonstrate the differences in the phase shift only the upper and lower halfes of each interferogram are shown and the evaluation is made at the intersection of the pictures. The interferograms show the heat and mass transfer boundary layer at a heated vertical wall with free convection. The mass transferred was naphtalene into air.

Heat and mass transfer experiments were also performed in a burning flame with hexane flowing out of a horizontal porous cylinder and oxidising after evaporation. Fig. 24 shows the two interferograms obtained with the two wave-lengths as emitted by the He-Ne-laser

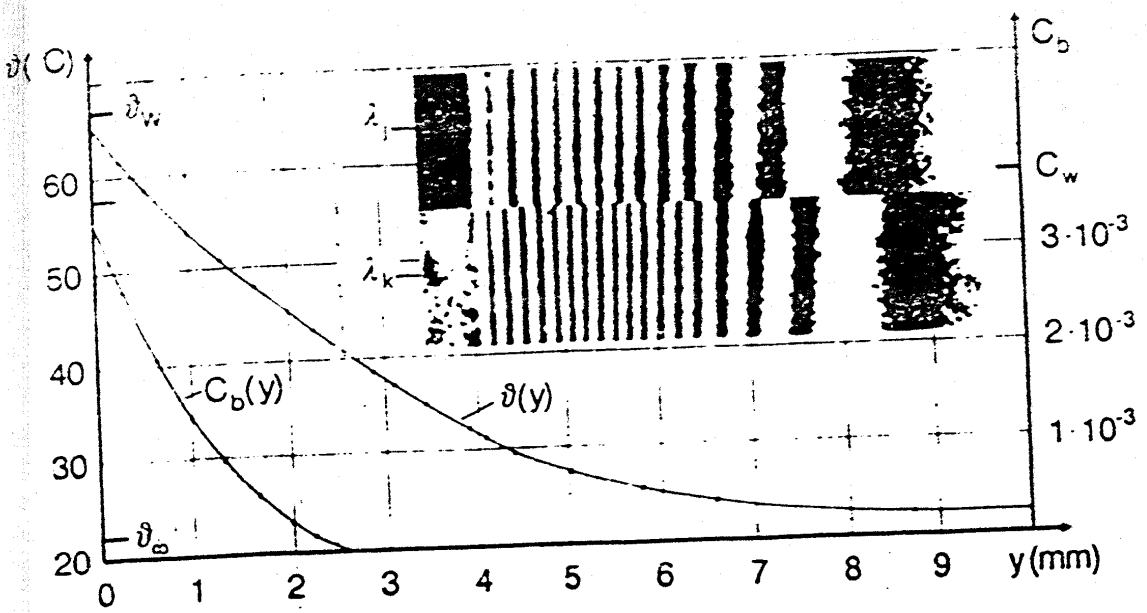

Fig. 23: Temperature and concentration profiles in a laminar boundary layer

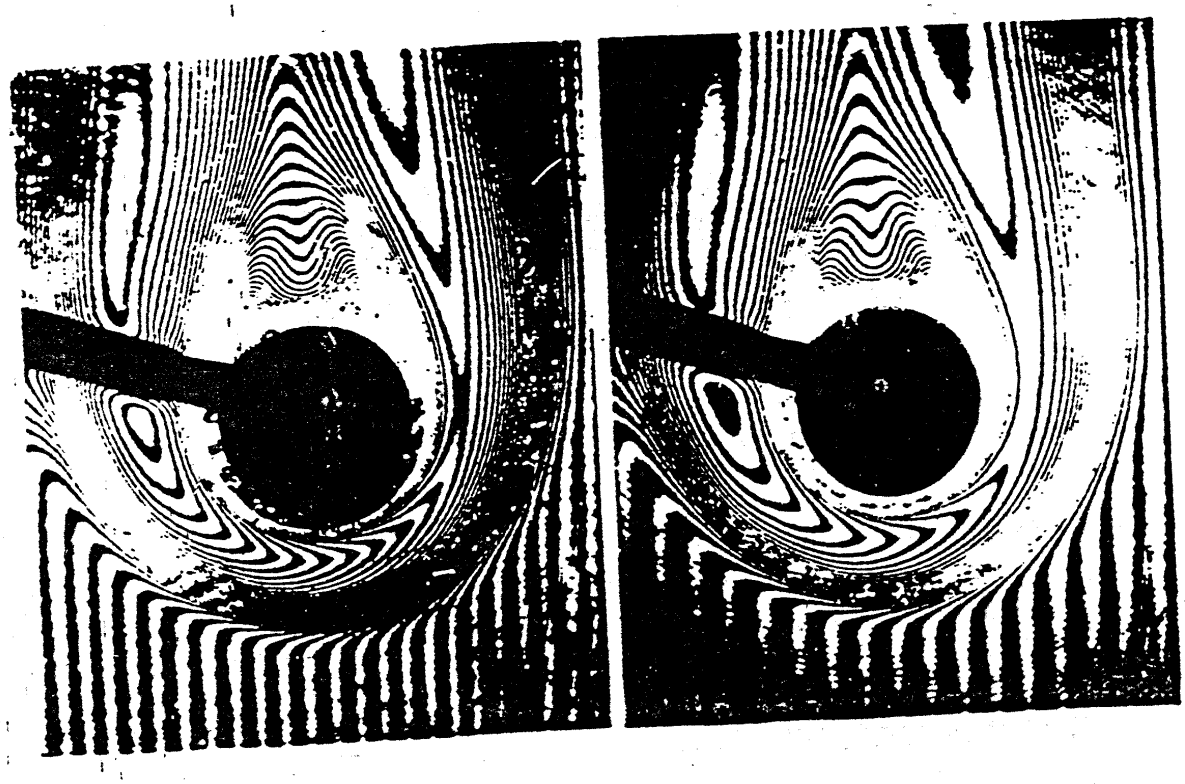

Fig. 24: Finite fringe interferogram of a flame taken with two different laser beams of the wavelength λ_j (right) and λ_k simultaneously

and the Argon-laser. In this interferogram the finite fringe method was used as described before. The temperature feld in this flame evaluated from the interferograms in Fig. 24 is given in Fig. 25, which clearly demonstrates the benefit of this optical method by

instantaneously presenting a complete information about the temperature distribution in the flame.

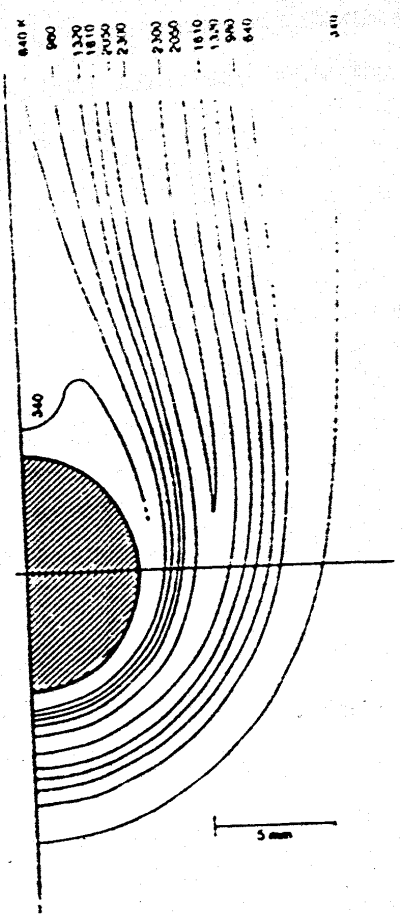

Fig. 25: Evaluation of the temperature field in a flame from the interferogram of Fig. 24

6. Concluding Remarks

Optical methods are expected to experience a powerfull revival due to three reasons: Sophisticated theoretical treatment of heat- and mass transfer processes with large computer codes needs very detailed information about temperature- and concentration-fields in the areas of interest like in boundary layers - for assessing and improving the physical models used in the code and for verifying the code itself. An optically determined pattern of isotherms is a very stringent touchstone for the reliability and accuracy of the code. Modern developments in power and process engineering make transient situations more and more interesting, especially for controlling procedures and safety deliberations. Optical measuring techniques work inertialess.

A former draw-back of the image-forming optical measuring techniques, the laborious and time consuming evaluation does not exist anymore. A personal computer can evaluate

a hologram or an interferogram within a few seconds which took manpowers of several hours before. The costs of such an evaluating equipment are relatively moderate. So theoretical analysis and optical measuring techniques could form a new phalanx for investigating heat and mass transfer processes.

7. Literature

1. **Arnold, C.D., Hewitt, G.F.**, Further developments in the photography of two-phase Gas liquid flow, Journal of photographic science 15, 97, 1967.
2. **Langner H.**, Untersuchungen des Entrainmentverhaltens in stationären und transienten zweiphasigen Gemischen, Diss. TU Hannover, 1978.
3. **Neumann, M.; Mayinger, F.**, Dust collection in Venturi-scrubbers, German Chemical Eng. 1, p. 289-293, 1978
4. **Gabor, D.**, A New Microscopic Principle, Nature 161, p. 777, 1948, Microscopy by Reconstructed Wavefonts, Proc. Rcy. Soc. A 197, p. 454, 1949, Microscopy by Reconstructed Wavefonts II, Proc. Phys. Soc. 3 64, p. 449, 1951.
5. **Kiemle, H., and D. Rõss (1969).**, Einführung in die Technik der Holographie, Akademische Verlagsgesellschaft, Frankfurt.
6. **Smith, H.M., (1969).**, Principles of holography, Wiley (Interscience), New York.
7. **Caulfield, H.J. and Sun Lu (1971).**,The applications of holography, Wiley (Interscience), New York.
8. **Chávez, A., Mayinger, F. (1990).**, Evaluation of pulsed laser holograms of spray droplets by applying image processing, 9th International Conference on Heat Transfer, 1990, p. 187.
9. **Chávez, A., Mayinger, F. (1992).**, Measurement of direct-contact condensation of pure saturated vapour on an injection spray by applying pulsed laser holography, Int. J. Heat Mass Transfer, Vol. 35 No. 3, pp 691-702, 1992.
10. **Mayinger, F., Panknin W. (1974).**, Holographie in Heat and Mass Transfer, 5th Int. Heat Transfer Conference, VI, 28, Tokio.
11. **Panknin, W. (1977).**, Eine holographische Zweiwellenlängen-Interferometrie zur Messung überlagerter Temperatur- und Konzentrationsgrenzschichten, Diss. Universität Hannover.
12. **Hauf, W., Grigull, U. (1970).**, Optical Methods in Heat Transfer, Advances in Heat Transfer, Vol. 6, p. 133.

13. **Hauf, W., Grigull, U., Mayinger, F. (1991).**, Optische Messverfahren in der Wärme- und Stoffübertragung, Springer Verlag, Berlin.

14. **Nordmann, D., Mayinger, F. (1981).**, Temperatur, Druck und Wärmetransport in der Umgebung kondensierender Blasen, VDI Forschungsh., Nr. 605, VDI Verlag, Düsseldorf.

15. **Chen, Y. M., (1985)**, Wärmeübergang an der Phasengrenze kondensierender Blasen, Diss. Techn. Universität München.

16. **El-Wakil, M.M., Myers, G.E., Schilling, R.J. (1966).**, An Interferometric Study of Mass Transfer from a Vertical Plate at Low Reynolds Numbers, J. of Heat Transfer, Vol. 88, p. 399.

17. **El-Wakil, M.M., Ross, P.A. (1960).**, A Two Wavelength Interferometric Technique for the Study of Vaporization and Combustion on Fuels, Liquid Rockets and Propellants, Progress in Astronautics and Rocketry, Vol. II, Academic Press, New York.